Water Science & Technology

 Water Science & Technology Vol 86 No 10, 2528 doi: 10.2166/wst.2022.358

Optimization of roughing filtration unit for a handwashing wastewater recirculation point-of-use system

Peter Wilberforce Olupot [a], Emmanuel Menya [a,b,*], Joseph Jjagwe [a], Joel Wakatuntu [a], Franz Román [c] and Oliver Hensel [c]

[a] Department of Mechanical Engineering, College of Engineering, Design, Art and Technology, Makerere University, P.O. Box 7062, Kampala, Uganda
[b] Department of Biosystems Engineering, Gulu University, P.O. Box 166, Gulu, Uganda
[c] Department of Agricultural and Biosystems Engineering, Faculty of Organic Agricultural Sciences, University of Kassel, Nordbahnhofstr, 1a, Witzenhausen 37213, Germany
*Corresponding author. E-mail: E.menya@gu.ac.ug

PWO, 0000-0003-4167-5306; EM, 0000-0002-4034-5308; JJ, 0000-0003-0819-8587; JW, 0000-0002-3328-7373

ABSTRACT

A downward roughing filter unit consisting of silica sand as the filter medium was optimized for performance towards removal of turbidity and suspended solids from handwashing wastewater. Design-Expert software was employed to optimize media particle size, filter depth, and flowrate. Linear and quadratic models were found to best fit the responses of turbidity and suspended solids removal, respectively. Particle size and flow rate were the only parameters with significant effects on removal of turbidity and suspended solids. Optimal conditions were found to be media particle size 0.6 mm, filter depth 12 cm, and flow rate 0.3 $Lmin^{-1}$, corresponding to removal efficiencies of 62 and 67% for turbidity and total suspended solids (TSS), respectively, as predicted by the model. Validation of model at optimal conditions resulted in turbidity and TSS removal of 55 and 53%, respectively. Additionally, removal efficiencies of the roughing filter towards apparent colour, true colour, biochemical oxygen demand (BOD_5), and chemical oxygen demand (COD) from handwashing wastewater were 56, 20, 32, and 5%, respectively. Overall, although turbidity of filtered water was >50 NTU, the reduction achieved by roughing filtration is a significant step in enhancing the performance of water treatment processes downstream, including filtration and adsorption by slow sand filters and activated carbon, respectively.

Key words: filtration, handwashing, recycling, roughing filter, wastewater

HIGHLIGHTS

- Downward roughing filter was optimized for pretreatment of handwash wastewater.
- RSM was employed to optimize filter media size, depth, and flowrate.
- Optimized system attained turbidity and TSS removal of 55 and 53%, respectively.
- Roughing filtration to enhance the performance of downstream treatment processes.
- Results contribute to design of treatment systems for onsite water recirculation.

GRAPHICAL ABSTRACT

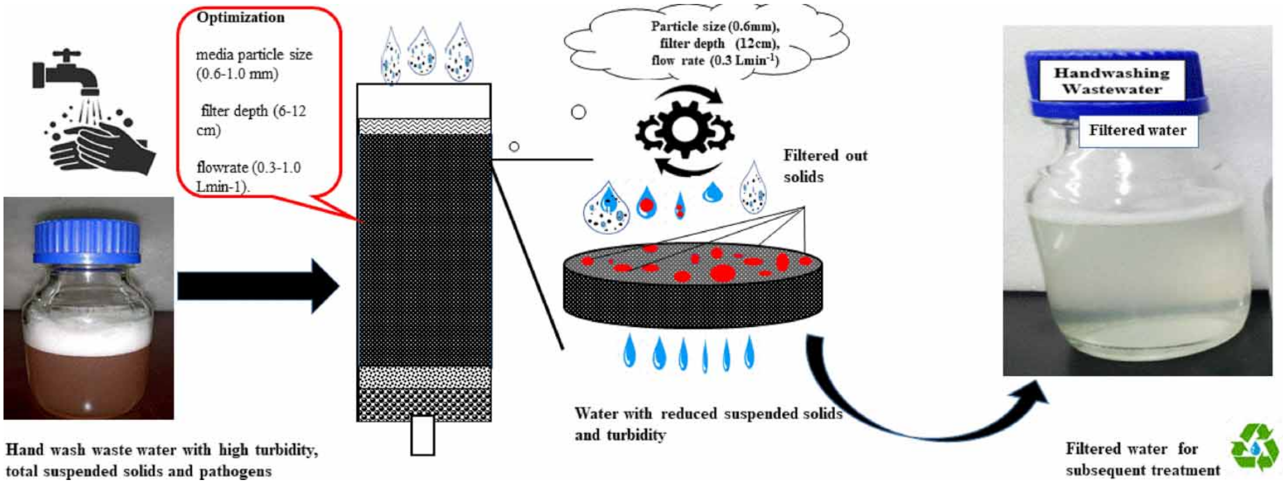

1. INTRODUCTION

The COVID-19 pandemic has intensified the importance of proper handwashing in curbing the spread of infectious diseases (Amuakwa-mensah *et al.* 2021; Chang *et al.* 2022; Wong *et al.* 2022). The correct hand washing technique, using clean water and soap has been demonstrated to be an effective preventive option. This is due to its low cost and user-friendliness (WHO 2020). Despite its importance, handwashing remains limited among some communities in developing countries, primarily due to water scarcity (Bukuluki *et al.* 2020; Alim *et al.* 2021). To provide such communities with an opportunity to practice handwashing, research efforts are geared towards development of treatment systems, where the handwashing wastewater can be treated and recycled (Ziemba *et al.* 2018; Subramanian *et al.* 2020; Olupot *et al.* 2021). Consequently, more users are able to practice handwashing, thus helping curb the spread of infectious diseases. Conventionally, domestic greywater treatment for reuse has been achieved by using a combination of materials such as: activated carbon, sand and gravel (Samayamanthula *et al.* 2019), activated carbon, zeolite and nano zero valent iron (Amiri *et al.* 2019), aluminum–iron electrodes (Barişçi & Turkay 2016) as well as sand, zeolite, pumice, and granular activated carbon (Bahrami *et al.* 2020). However, these approaches are limited by high initial costs involved, requirement of spacious facilities, and regular replacements due to clogging. A roughing filter could be employed in the pretreatment stage for reduction of influent turbidity and suspended solids, which are otherwise responsible for clogging of slow sand filters, and thus their shorter filter runs. According to Wegelin & Schertenleib (1993), roughing filtration can achieve filter runs that are five times longer than when slow sand filters are run without prior roughing filtration. Moreover, with longer filter runs, the need for frequent cleaning of the slow sand filter is reduced, allowing enough time for biological maturation between cleaning sessions, which would otherwise lead to an increased risk of pathogen breakthrough (Cleary 2005). The range of source water quality that can be successfully treated using slow sand filters is also widened once roughing filtration of the influent is employed as a pretreatment stage for slow sand filtration (Logsdon *et al.* 2002). However, roughing filtration systems should only be deployed for influent turbidity >50 NTU (WHO 2008) or if the suspended solids take more than 6–8 h to settle out to obtain a supernatant with turbidity <5 NTU (Oxfam 2001). In other studies (Wegelin 1996; Oxfam 2001), the levels of turbidity and total suspended solids (TSS) desired of the effluent from a roughing filtration system are even more stringent. For instance, Wegelin (1996) reported that roughing filters should aim at producing water with a turbidity and TSS concentration of 10–20 NTU and $\leq$2–5 mgL^{-1}, respectively, if water is to be subsequently passed through a slow sand filter. Oxfam (2001) reported that the turbidity of the effluent should be $\leq$5 NTU if the water is to be disinfected with chlorine.

Roughing filters employ multiple grades of filter media materials that decrease successively in size in the direction of water flow. The use of multiple grades of filter media promotes penetration of particles throughout the filter bed, taking advantage of large storage capacities offered by larger filter media materials, and higher removal efficiencies offered by smaller filter media materials (Nkwonta *et al.* 2010; Maciel *et al.* 2021). The use of multiple grades of filter media also allows attainment of treatment targets by a shorter filter than when a longer filter packed with one media size is used (Nkwonta 2010). Roughing filters employ screening, sedimentation, and interception to separate solids from raw water. During the screening process, particles such as leaves, small stones, and debris larger than the pore size of the filter media are screened out of the water. During the sedimentation process, the settle-able particles are separated from water, while during interception, particle removal is enhanced through a gradual reduction of the pore size caused by accumulated material (Wegelin 1996; Matuzahroh *et al.* 2020). With these removal mechanisms, roughing filters have been reported to reduce turbidity and suspended solids with efficiencies as high as 86 and 85%, respectively (Mushila *et al.* 2016). Elsewhere, turbidity removal efficiencies ranging from 30 to 90% have been reported (Hasnain & Khan 2014; Karki & Amatya 2020; Cahyana *et al.* 2021)

Besides solids separation, roughing filters can improve the microbial quality of water (Nouri *et al.* 2008). For instance, Matuzahroh *et al.* (2020) reported a coliform removal efficiency ranging from 90 to 93.91%. However, due to potentially larger pore size of the filter media, roughing filters are sometimes not effective at removing bacteria from water. This is due to the smaller size of bacteria that allows them to evade the screening process (Matuzahroh *et al.* 2020). Other water quality parameters that can be improved by the roughing filter include colour, dissolved organic matter, nutrients, heavy metals, and chemical oxygen demand (COD) (Lee & Jayalath 1998; Nkwonta & Ochieng 2009; Nkwonta 2010; Munasir *et al.* 2015).

Despite the significant progress made towards the development of handwash-wastewater treatment systems (Nguyen *et al.* 2017; Ziemba *et al.* 2018; Olupot *et al.* 2021), the roughing filtration system, which in some scenarios forms part of the treatment system, has not yet been optimally configured. Consequently, turbidity and suspended solids in effluents from the roughing filtration systems are not sufficiently reduced to levels required for successful operation of the slow sand filtration systems. For instance, in a study by Olupot *et al.* (2021), after the roughing filtration stage, the turbidity and TSS of the influent to the slow sand filter were found to be 204–266 NTU and 404–426 mgL^{-1}, translating to removal efficiencies of 8.89–13.11 and 9.68–14.35%, respectively. The remaining turbidity and suspended solids compromise the performance of the slow sand filtration system for reasons already cited above. Moreover, unlike elsewhere, roughing filters have been employed to treat raw surface water for meeting drinking water requirements (El-taweel & Ali 2000), as well as to treat greywater from the kitchen, laundry, and bathing for non-potable reuse applications (Bakare *et al.* 2019). Very scant information is available concerning optimization of the roughing filtration systems for wastewater generated from handwashing alone. This study adopted the robustness of response surface methodology (RSM) to optimize the configuration of a roughing filtration system. The removal of the influent turbidity and suspended solids was improved to allow adequate slow sand filter operation. More specifically, the downward vertical roughing filtration system was considered due to its relatively lower cost and space requirement than the horizontal filtration system. Moreover, though the vertical roughing filter may undoubtedly need more frequent cleaning than the horizontal roughing filter, cleaning of roughing filters is neither labour nor energy intensive (Cleary 2005). Furthermore, a downward filter does not require a pump during operation as compared to upward-vertical and horizontal roughing filters. Therefore, this study sought to optimize the performance of a downward vertical roughing filter in the pretreatment of handwashing with high values of turbidity and total suspended solids. The filtration parameters that were optimized include the filter media particle size, filtration flow rate, and the filter media depth.

2. MATERIALS AND METHODS

2.1. Filter media materials

Materials for the filter media included silica sand and gravel due to their indispensable properties and abundant availability. These were sourced from one of the sand mines found in Wakiso district, Uganda. To remove impurities from the sourced samples, each of the samples was washed with both tap and de-ionized water, followed by oven-drying at 105 °C for 24 h. The oven-dried samples were then reduced in size using a mallet hammer, a ball mill, and a mortar and pestle. The resultant particles corresponding to each of the filter media were sieved to obtain sizes ranging from 5 to 50 mm, followed by storage in airtight polythene bags.

2.2. Filter media characterization

The finest silica sand particles were characterized using X-ray fluorescence (XRF) spectroscopy and scanning electron microscopy (SEM) techniques. XRF and SEM were employed to obtain the chemical composition and morphology of the filter media materials, respectively. The procedures reported by Olupot *et al.* (2021) were followed in this study. More specifically, for XRF, a handful sample of silica sand was initially pulverized in a Hazorg mill to obtain a powdered sample, from which a 1 g sample was drawn and subsequently mixed with 7 g of lithium bromide (LiBr) in a gold platinum mould. The resultant sample was burnt on an XRF bead maker at 750 °C, followed by cooling and analysis in an XRF cassette calibrated with different materials. To obtain loss on ignition (LOI), about 2 g of each sample material was burnt in a muffle furnace at 950 °C (Oyedotun 2018).

For SEM, the field emission scanning electron microscope (Tescan Vega 3, Pleasanton, USA) was employed to determine the morphology of silica sand. This involved fixing the silica sand on a double-sided adhesive carbon tape, followed by vacuum drying, and then scanning at an acceleration voltage of 10 kV.

2.3. Collection and characterization of raw handwashing wastewater

Samples of raw handwashing wastewater were collected from five handwashing stations instituted at public facilities in Kampala City, Uganda. These stations have been defined by Olupot *et al.* (2021). From each station, four samples were collected, and these were mixed to form a single homogenous sample which was subsequently assessed in triplicates for the most important water quality parameters which influence the design of water treatment plants. The parameters included true colour, turbidity, suspended solids concentration, and degree of faecal pollution. Determination of true colour involved initially filtering the water samples through a Whatman filter (GF/C 47 mm diameter, and 1.2 μm pore size), followed by analyzing the filtrate for true colour based on the platinum cobalt standard method (APHA 2012). Turbidity was determined based on the absorptometric method 8237 with measurements made at a wavelength of 450 nm using a spectrophotometer (HACH DR 2000). TSS was determined based on the HACH standard: Photometric Method 8006 (APHA 2012). The degree of faecal pollution was determined based on the concentrations of *E.coli* and total coliforms (CFU/100 mL) using the spread plate count method (APHA 2012).

2.4. Roughing filter type

A downward roughing filter type was adopted in this study. The selection of this filter type was based on the fact that it does not require a pump under normal operation and its operational costs are very minimal compared to upward vertical and horizontal rouging filters. However, it should be noted that for experimental runs in this study, a peristaltic pump was used to regulate the flow rate of wastewater into the filtration column. Silica sand particles were packed in the filtration column in order of decreasing particle sizes from bottom to top. The top most layer of sand particles at a given time was considered the filter depth and assessed for performance, while the rest of the sand particles served as support materials. Polyvinyl chloride tube with a height and internal diameter of 300 and 100 mm, respectively, was used to construct the filter column. Two perspex circular plates were uniformly perforated with 0.5 mm holes onto their surfaces. One such plate was fitted at the top of the set up, while the other was placed at the bottom as illustrated in Figure 1(a). The top plate acted as a distribution surface to spread the influent water stream into the filter column thus avoiding preferential flow. The bottom plate was used to hold the filtration media. Figure 1(b) shows the filtration setup that was employed in the optimization studies.

2.5. Optimization of the filter configuration

Optimization studies were tailored to the finer filter sand media material on the assumption that handwashing wastewater does not contain larger solids materials that would otherwise need to be trapped and stored in gravel and/or in the filter

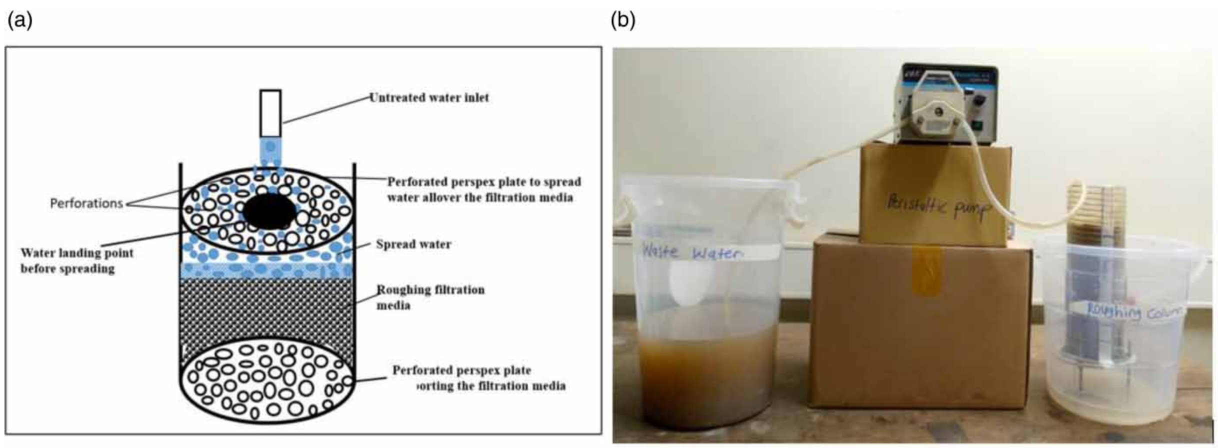

Figure 1 | (a) Unit column with perspex plates. (b) Roughing filtration setup employed in the optimization studies.

medium of intermediate size. The particle size and filter depth of the finer filter media ranged from 0.6 to 1.0 mm and 6.0 to 12.0 cm, respectively, as informed by Olupot *et al.* (2021). These, together with a flow rate of 0.3–1.0 $Lmin^{-1}$, were optimized using a response surface methodology (RSM) design called central composite design (CCD).

2.5.1. Design of experiments

Particle size (P), filter depth (D), and flow rate (R) were the three input variables employed in a 3-factor, 2-level CCD. Table 1 shows the low and high levels of each factor denoted as −1 and +1, respectively.

The input variables and their ranges were selected based on an earlier study by Olupot *et al.* (2021). Twenty (20) experimental runs were executed using Design-Expert software (version 13, Stat-Ease Inc., MN, USA) in a randomized order to minimise the effects of uncontrolled factors. The runs comprised 8 factorial points, 6 axial points, and 6 replicates at the centre points as determined from Equation (1). The centre points determined experimental error and reproducibility of the data.

$$N = 2^n + 2n + n_c = 2^3 + 2(3) + 6 = 20 \quad (1)$$

where N is the total required experiments, n is the total process variables, and n_c represents replicates at the center points.

2.5.2. Development of an empirical model

For the model, removal efficiencies of suspended solids and turbidity by the developed roughing filter were optimized responses. The relationship between the input variables and the target responses was mathematically modeled using a polynomial Equation (2).

$$Y = b_o + \sum_{i=1}^{n} b_i X_i + \sum b_{ii} X_i^2 + \sum_{i=1}^{n-1} \sum_{j=i+1}^{n} b_{ij} X_i X_j + \varepsilon \quad (2)$$

where Y is the response (either turbidity or total suspended solids contents), X_i and X_j are the independent variables (particle size, filter depth, and flow rate), b_o, b_i, b_{ii}, b_{ij} represent the constant, linear, quadratic, and interaction coefficients, respectively, while ε is the error of the model.

The goodness of fit of data to the developed models was evaluated based on coefficient of determination (R^2), predicted R^2-value, adjusted R^2-value, adequate precision, and coefficient of variation (CV) values. Adequate precision was an indicator of signal to noise ratio, while CV was a determinant of the reproducibility of the models. Fisher's F-test was used to determine the statistical significance of developed models and regression coefficients at 95% confidence level. Variation of data around the fitted model and associated statistical significances were evaluated using the lack of fit F-test. Results of the evaluation of lack of fit F-test were presented as the probability of lack of fit (p-values of lack of fit). The insignificant model terms were eliminated by a backward selection at an alpha value of 0.10. These terms would increase the R^2-value, and consequently indicate inaccurate regression models.

2.5.3. Optimization and model validation

The targeted criterion was to maximize each of the studied responses within the predetermined ranges of filtration process parameters (particle size, filter depth, and flow rate). Design-Expert software explored a combination of factors that simultaneously satisfied the requirements placed on each of the responses and factors. The developed response surface models

Table 1 | Experimental values used in the central composite design of Design-Expert software

Factor	Filtration parameter	Units	Low (−1) value	High (+1) value
P	Particle size	mm	0.6	1.0
D	Filter depth	cm	6.0	12.0
R	Flow rate	$Lmin^{-1}$	0.3	1.0

were validated by conducting the respective experiments under optimum filtration conditions. The obtained experimental values were then compared with the values predicted by the model.

2.5.4. Further performance analysis

The optimized roughing filter configuration was further evaluated towards removal of additional parameters from handwashing wastewater, including pH, apparent colour, true colour, biochemical oxygen demand (BOD_5), and COD. pH was determined using a portable meter (HQ 30d Flexi). BOD_5 was determined based on the BOD track method (APHA 2012). In this method, water samples were put in 300 mL incubation bottles and seeded with microorganisms, followed by a determination of the initial dissolved oxygen (DO) concentration. The incubation bottles with the water samples were then sealed, and incubated at 20 °C for five days in the dark, followed by a determination of the final DO concentration. The difference between initial and final DO readings was determined and corrected for BOD_5 of the seed and dilution factor. The corrected value was obtained as the BOD_5 of the water sample. COD of water samples was determined based on the closed reflux titrimetric method (APHA 2012).

3. RESULTS AND DISCUSSION

3.1. Characteristics of silica sand

3.1.1. Chemical composition

The XRF results (Table 2) showed that SiO_2 was the major component in silica sand employed in this study. These findings corroborate those reported elsewhere (Table 2). It is desirable to have silica (SiO_2) content greater than 90% for sand to be suitable for water filtration (Aba *et al.* 2019). Thus, the sand used in this study could serve the purpose of water filtration.

3.1.2. Morphology of the filter media material

The morphology of the finest filter sand media material before and after roughing filtration at the optimal conditions was obtained by SEM. As earlier stated under Section 2.5, due to the absence of larger solids materials in the handwashing wastewater, it was hypothesized that the majority of the solids were filtered in the finest filter media material. Therefore, this media material was of great interest to visualize the morphology of the sand before and after filtration (see Figure 2). The non-porous rough surface with a block-like structure (Figure 2(a)) is common with siliceous sand particles, as reported by Rey *et al.* (2021). Figure 2(b) shows that the surface of the filter media was covered with a white homogenous, smooth layer as opposed to the initial morphology (Figure 2(a)), suggesting that the removal of pollutants may be caused by filtration and/adsorption of surfactant molecules.

3.2. Characteristics of handwashing wastewater

The characteristics of the homogenous handwashing wastewater obtained from different handwashing stations is shown in Table 3. Besides pH, the levels of turbidity, total suspended solids, true colour, *E.coli,* and total coliform were all above the levels permissible for wastewater discharge to the environment in the Ugandan context (NEMA 1999). The presence of *E.coli* and coliforms in wastewater suggested presence of pathogens, which pose health risks to animals and humans upon contact with the wastewater (Luna-Guevara *et al.* 2019; Ratna 2019). A turbidity of the handwashing wastewater greater than 50 NTU points to the need for roughing filtration to remove suspended solids, if frequent clogging of the slow sand filter is to be avoided (WHO 2008).

Table 2 | Chemical composition of silica sand used in this study for construction of the roughing filter

Reference	SiO_2	Al_2O_3	Fe_2O_3	CaO	MgO	SO_3	K_2O	Na_2O	LOI
This study	97.92	0.02	1.50	0.40	0.00	0.01	0.06	0.00	0.10
Alftessi *et al.* (2021)	99.50	0.36	0.09	0.01	–	0.01	0.00	–	–
Aba *et al.* (2019)	98.68	–	0.39	0.19	–	–	0.44	–	–
Setiati (2017)	96.50	2.15	0.33	0.03	0.09	0.00	0.22	0.23	–

Note: *LOI* is loss on ignition.

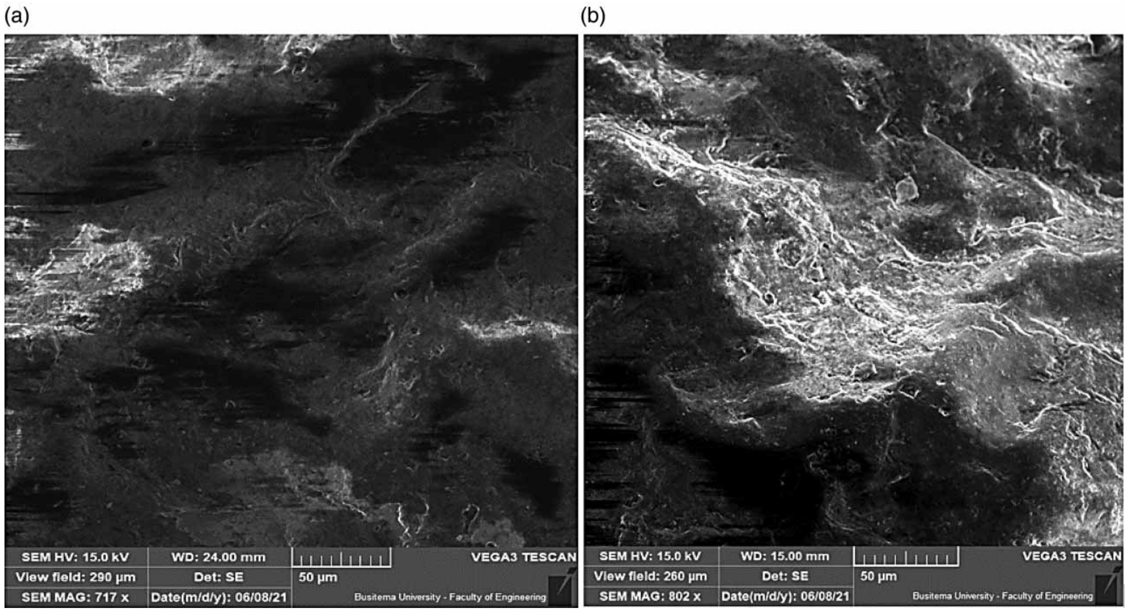

Figure 2 | SEM images for (a) the raw sand before roughing filtration, and (b) the sand after roughing filtration of the handwashing wastewater.

Table 3 | Characteristics of handwashing wastewater as obtained from different public handwashing stations

Parameter	Value	NEMA effluent discharge Standards[a]
pH	6.62 ± 0.48	6.0–8.0
Turbidity (NTU)	775 ± 38	300
Total suspended solids (mg/L)	288.8 ± 19.67	100
True colour (PtCo)	7,581 ± 359	300
Apparent colour (PtCo)	8,508.6 ± 373	–
E.coli (CFU(100 mL)$^{-1}$)	2,543 ± 124	ns
Total coliforms (CFU(100 mL)$^{-1}$)	13,935 ± 2,042	5,000

Note: (i) NEMA stands for National Environment Management Authority of Uganda, and (ii) [a]indicates Uganda's national effluent discharge standards, 1999.

3.3. Development of regression model equations

The correlations between the selected filtration parameters (particle size, filter depth, and flow rate) and the responses (turbidity removal and suspended solids removal) were established using the CCD. The experimental design and corresponding experimental values for each of the responses are shown in Table 4.

From Table 4, turbidity and suspended solids removal values ranged from 22 to 66% and 23 to 71%, respectively. The sequential model sum of squares was considered to find the best fit for each response (see Table 5). The highest order polynomial, where the additional terms are significant, and the model is not aliased, was suggested by the Design-Expert software and consequently selected.

The linear and quadratic models were found to best fit the responses of turbidity and suspended solids removal, respectively. In terms of coded factors, the response surface reduced linear and quadratic models corresponding to turbidity removal (Y_1) and suspended solids removal (Y_2), after excluding the insignificant terms are given in Equations (3) and (4), respectively.

$$Y_1 = 46.50 - 9.01A - 6.75C \quad (3)$$

$$Y_2 = 51.77 - 9.70A + 2.79B - 7.68C - 5.24A^2 \quad (4)$$

Table 4 | CCD and experimental results

Run	Filtration parameters			Responses	
	A **(particle size, mm)**	***B*** **(filter depth, cm)**	***C*** **(flow rate, Lmin^{-1})**	***Y_1*** **(turbidity removal, %)**	***Y_2*** **(suspended solids removal, %)**
1	0.6	6	1.00	44.91	47.44
2	1.0	12	1.00	22.97	26.59
3	0.8	9	0.65	36.69	39.51
4	0.8	9	0.65	45.14	46.95
5	0.8	9	0.65	45.71	49.02
6	0.8	9	0.65	48.34	52.32
7	1.0	6	1.00	28.12	25.29
8	0.6	12	1.00	61.12	62.15
9	0.8	4	0.65	44.69	46.34
10	0.8	9	1.24	41.83	41.95
11	0.8	14	0.65	50.74	52.80
12	1.0	12	0.30	45.83	49.63
13	0.8	9	0.65	50.51	53.90
14	0.5	9	0.65	49.78	47.60
15	1.0	6	0.30	43.47	41.98
16	0.6	12	0.30	63.27	64.96
17	0.8	9	0.65	56.11	59.63
18	1.1	9	0.65	28.12	23.80
19	0.6	6	0.30	57.71	61.34
20	0.8	9	0.06	65.03	70.73

Table 5 | Sequential model sum of squares for turbidity removal (a) and suspended solids removal (b)

Source	**Sum of squares**	**df**	**Mean square**	***F*-value**	***p*-value (Prob > F)**	**Remarks**
(a) Sequential model sum of squares for turbidity removal efficiency						
Mean vs total	43,253.37	1	43,253.37			
Linear vs mean	1,793.05	3	597.68	14.13	0.0001	Suggested
2FI vs linear	144.26	3	48.09	1.17	0.3575	
Quadratic vs 2FI	215.90	3	71.97	2.27	0.1424	
Cubic vs quadratic	106.33	4	26.58	0.7585	0.5882	Aliased
Residual	210.28	6	35.05			
Total	45,723.19	20	2,286.16			
(b) Sequential model sum of squares for suspended solids removal efficiency						
Mean vs total	46,458.05	1	46,458.05	12.86		
Linear vs mean	2,195.50	3	731.83	0.42	0.0002	
2FI vs linear	80.05	3	26.68	4.51	0.7434	
Quadratic vs 2FI	477.61	3	159.20	0.76	0.0301	Suggested
Cubic vs quadratic	119.18	4	29.79	12.86	0.5850	Aliased
Residual	233.85	6	38.98	0.42		
Total	49,564.25	20	2,478.21	4.51		

where A and B are particle size and filter depth in cm, while C is the flow rate in $Lmin^{-1}$. The positive sign (+) indicates a synergistic effect, while the negative sign (–) indicates the antagonistic effect of the factor on the given response.

3.4. Analysis of variance

ANOVA was employed to test for statistical significance of the developed regression models, model coefficients, and the model lack of fits. The results of ANOVA are summarized in Table 6. The model F-values of 19.91 and 19.18, corresponding to the reduced linear and quadratic models for turbidity and suspended solids removal, respectively, implied that the developed models were significant (p-values < 0.05). There was only a 0.01% chance that a model F-value this large could occur due to noise for each of the developed models. Additionally, the lack of fits for the developed models was not significant (p-value > 0.05), further suggesting that the developed models fit the experimental data well (Menya *et al.* 2019).

Model terms were significant for p-values < 0.05 and not significant for p-values > 0.10. Based on this, the significant terms were found to be A and C for the reduced linear model corresponding to turbidity removal. Out of these terms, the main effect of particle size (A) with F-value of 25.50 was found to have the most significant influence on turbidity removal from hand-washing wastewater, followed by flow rate (C) with F-value of 14.31. On the other hand, the main effect of filter depth (B) did not significantly influence turbidity removal, since its associated p-value was greater than 0.01.

The significant terms for the response surface reduced quadratic model corresponding to suspended solids removal include A, B, C and, A^2 (Table 6). Out of these terms, the main effect of particle size (F-value 37.93) was found to be the most significant factor influencing suspended solids removal, followed by the main effect of flow rate (F-value 23.77), and lastly, the quadratic effect of particle size (F-value 11.90). The main effect of filter depth did not significantly influence turbidity removal, since its associated p-value was greater than 0.01.

The goodness of fit of the developed models was evaluated based on standard deviation, R^2-value, adjusted R^2-value, predicted R^2-value, and adequate precision (see Table 7). The slight standard deviation from each developed model, suggests that the developed models are good. The relatively high R^2-values indicate that the data satisfactorily fits the developed models. More importantly, the adjusted and predicted R^2-values corresponding to each response were in reasonable agreement as their difference was <0.2. Adequate precisions (signal to noise ratio) due to each of the developed models were found to be greater than 4, suggesting that the developed models could be employed to navigate the design space.

Table 6 | ANOVA for response surface reduced models for turbidity and suspended solids removal

Source	Sum of squares	df	Mean square	F-value	p-value (Prob > F)	Remarks
(a) ANOVA for response surface reduced linear model for turbidity remo						
Model	1,730.81	2	865.41	19.91	<0.0001	Significant
A-particle size	1,108.65	1	1,108.65	25.50	<0.0001	
C-flow rate	622.16	1	622.16	14.31	0.0015	
Residual	739.01	17	43.47			
Lack of fit	530.52	12	44.21	1.06	0.5120	Not significant
Cor total	208.49	5	41.70			
(b) ANOVA for response surface reduced quadratic model for suspended solids removal						
Model	2,598.31	4	649.58	19.18	<0.0001	Significant
A-particle size	1,284.10	1	1,284.10	37.93	<0.0001	
C-flow rate	804.86	1	804.86	23.77	0.0002	
A^2	402.81	1	402.81	11.90	0.0036	
Residual	507.89	15	33.86			
Lack of fit	274.55	10	27.45	0.5883	0.7779	Not significant
Cor total	233.34	5	46.67			

Table 7 | Model summary statistics indicating goodness of fit of the developed models

Statistical parameter	Turbidity removal (%)	Suspended solids removal (%)
Standard deviation	6.59	5.82
Mean	46.50	48.20
R^2-value	0.70	0.84
Adjusted R^2-value	0.66	0.79
Predicted R^2-value	0.55	0.70
Adequate precision	12.34	15.83

3.5. Diagnostics and adequacy checking

Figure 3 shows the normal probability plots of externally studentized residuals, predicted versus actual values of the responses, as well as plots of externally studentized residuals versus predicted values. These plots were employed to check the adequacy of the fitted models.

Figure 3(a) and 3(b) show that the points on the normal probability plots conform to a straight line, confirming normal distribution of the data (Menya *et al.* 2019). The plots of predicted versus actual values of turbidity removal and suspended solids removal shown in Figure 2(c) and 2(d), respectively, show minimal divergence of points from the straight line, suggesting that the developed models can be employed to adequately represent the functional relationship between the experimental factors and the response variables. The plots of externally studentized residuals versus predicted values for turbidity

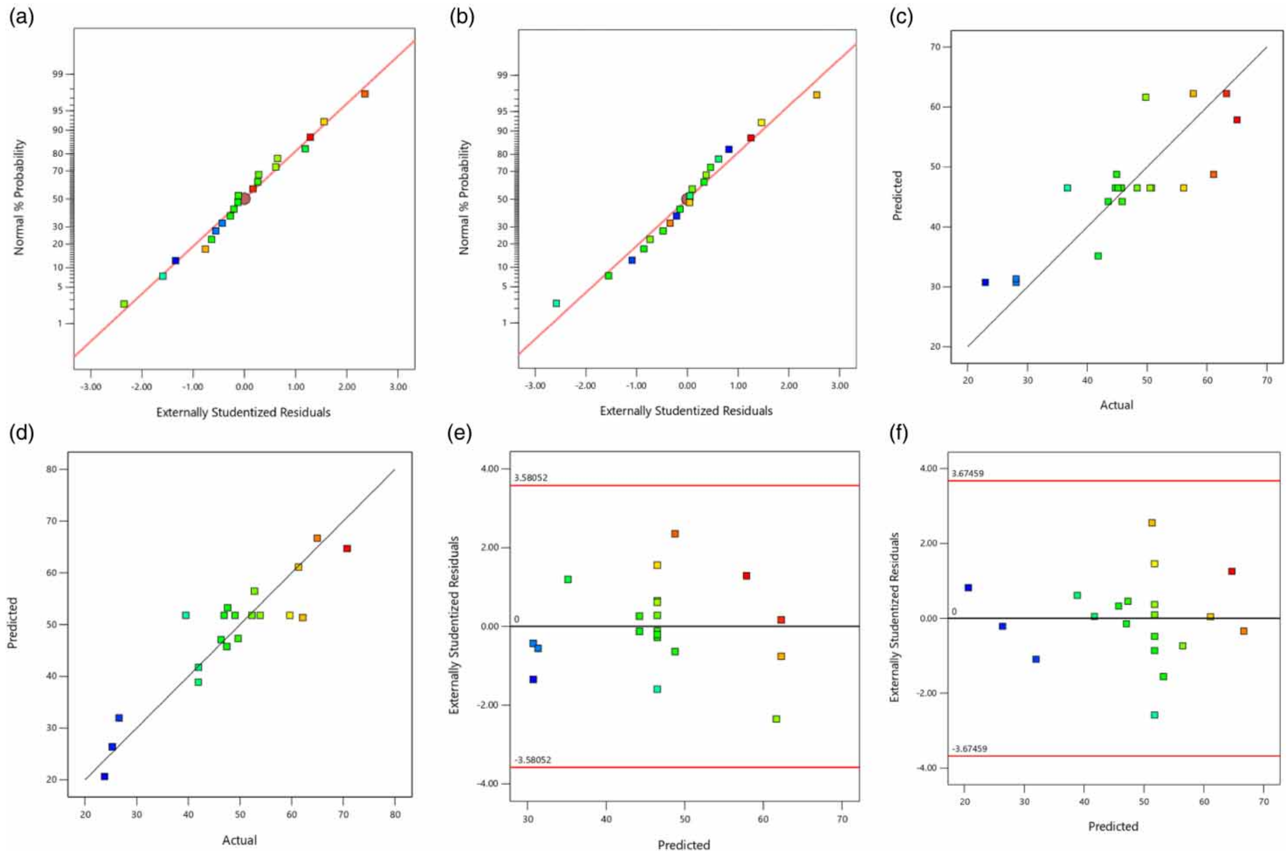

Figure 3 | Normal probability plot of residues for turbidity removal (a) and suspended solids removal (b); predicted values versus experimental values for turbidity removal (c), and suspended solids removal (d); residues versus predicted for turbidity removal (e), and suspended solids removal (f).

removal (Figure 3(e)) and suspended solids removal (Figure 3(f)) do not show any particular pattern, suggesting random distribution of the residues; a requirement for a good model. The plots of studentized residual versus run number (Figure 4) did not show any particular pattern, suggesting good data distribution. Moreover, each data was distributed within the acceptable limits, suggesting no constant error was detected (Talib *et al.* 2017).

3.6. Response surfaces

3.6.1. Turbidity removal

Figures 5(a)–5(d), respectively, show the three-dimensional (3D) and two-dimensional (2D) response surfaces plotted to show the interactive effects between filtration parameters on the removal of turbidity using the optimized roughing filtration system. Referring to the 3D surface plots, it can be seen that turbidity removal increased with a decrease in flow rate and particle size. This tendency may be attributed to the increased removal of matter such as silt, oils, food particles and other inorganic and organic matter deposited in water during handwashing (Nkwonta 2010). Decreased flow rate and particle size offer resistance to penetration of solid particles, thus high removal efficiency (Bakare *et al.* 2019; Dashti *et al.* 2019). Low flow rates allow water to have more interaction time with the filter media hence better removal of impurities which clears the water for reduced turbidity (Khan & Farooqi 2011; Karki & Amatya 2020). From the 2D contour plot (Figure 5(d)), it can be seen that filter depth did not have an influence on turbidity removal, affirming the results already obtained from the ANOVA (see Section 3.3). Moreover, the straight contour lines confirm a first-order regression model, where only the main effects of the filtration parameters had a significant influence on turbidity removal (Antony 2014). The interactive effects between the filtration variables did not, therefore, have significant influence on turbidity removal.

3.6.2. Suspended solids removal

Figure 6(a)–6(d) shows the 3D and 2D contour response surfaces plotted to show the interactive effects between filtration parameters on the removal of suspended solids using the optimized roughing filtration system. Referring to the 3D surface and 2D contour plots, it can be seen that suspended solids removal increased with a decrease in flow rate and particle size. This tendency may be attributed to smaller sand particle sizes having a lower porosity than larger ones, hence retaining an increased volume of solid matter (Nkwonta & Ochieng 2009). Lower flow rates also prevent penetration of coarse solid particles through the filter bed and increase the retention time, thus offering better removal efficiencies (Nkwonta 2010). Further looking at the 2D contour plots, it can be seen that filter depth did not have a significant influence on suspended solids removal (Figure 6(d)), affirming the results already obtained from the ANOVA (see Section 3.3). The non-straight

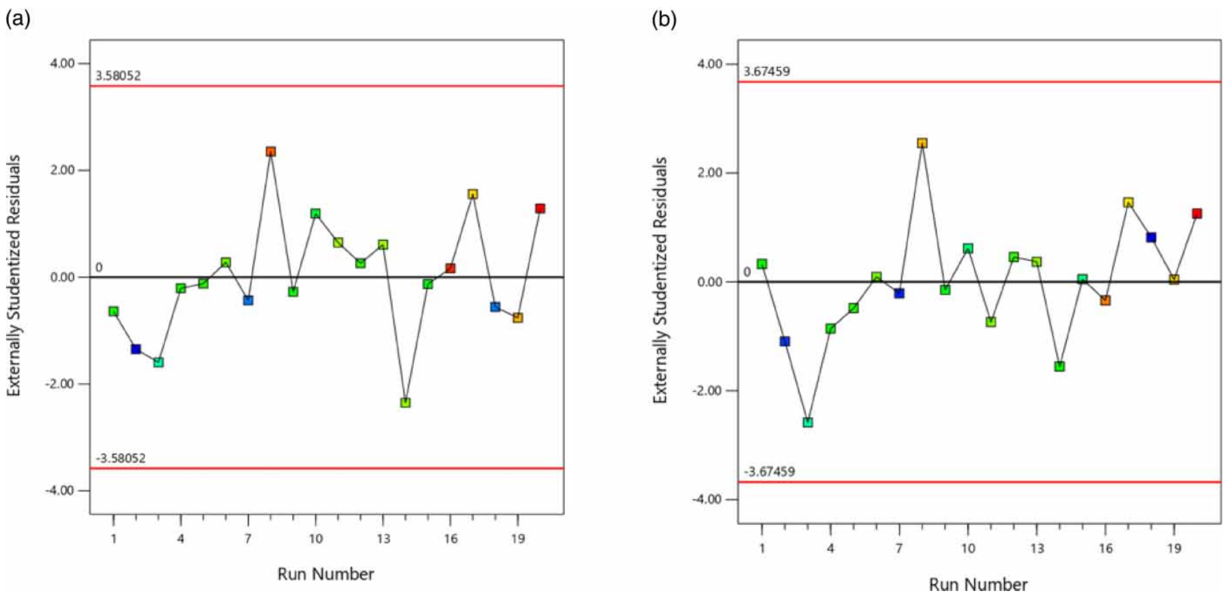

Figure 4 | Residual *vs* run number for turbidity removal (a) and suspended solids removal (b).

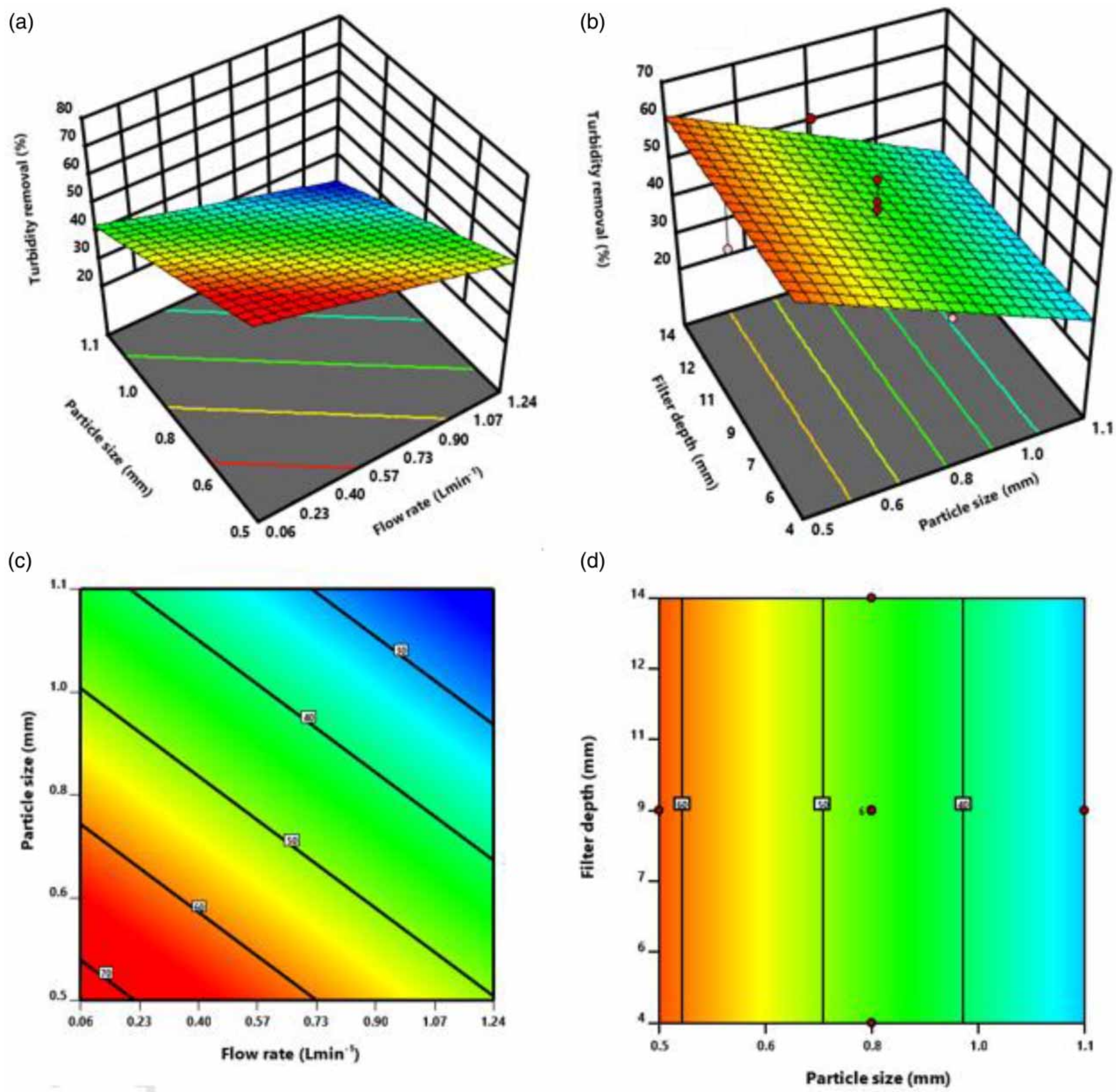

Figure 5 | Three-dimensional response surface plots of turbidity removal. (a) Effect of particle size, flow rate, and filter depth fixed at 9 cm. (b) Effect of particle size, filter depth, and flow rate fixed at 0.65 $Lmin^{-1}$. Two-dimensional contour plots of turbidity showing (c) interaction of flow rate and particle size (d) interaction of particle size and filter depth.

contour lines confirmed a second-order regression model (Antony 2014), which corroborates with the results obtained from the ANOVA.

3.7. Process optimization and validation

From model simulation using the numerical optimization method of the Design-Expert software, the optimum roughing filtration conditions were suggested as follows: filter media particle size (0.6 mm), filter depth (12 cm), and flow rate (0.3 $Lmin^{-1}$). Suppose filtration through the roughing filter was done under these conditions. In that case, the turbidity and suspended solids removal as predicted by the respective developed models are 62 and 67%, respectively, as indicated in Figure 7. Moreover, desirability of 0.924 indicated that over 92.4% of the optimization goals were satisfied by this solution.

To verify the predictive capability of the developed models, the roughing filtration system under the optimum conditions suggested the above was assessed for removal of turbidity and suspended solids from handwashing wastewater. The resultant removal efficiencies were subsequently compared with the values predicted by the respective models. As a rule of thumb, the mean experimental values should lie within the range of 95% prediction interval (PI) low and 95% PI high for a reliable

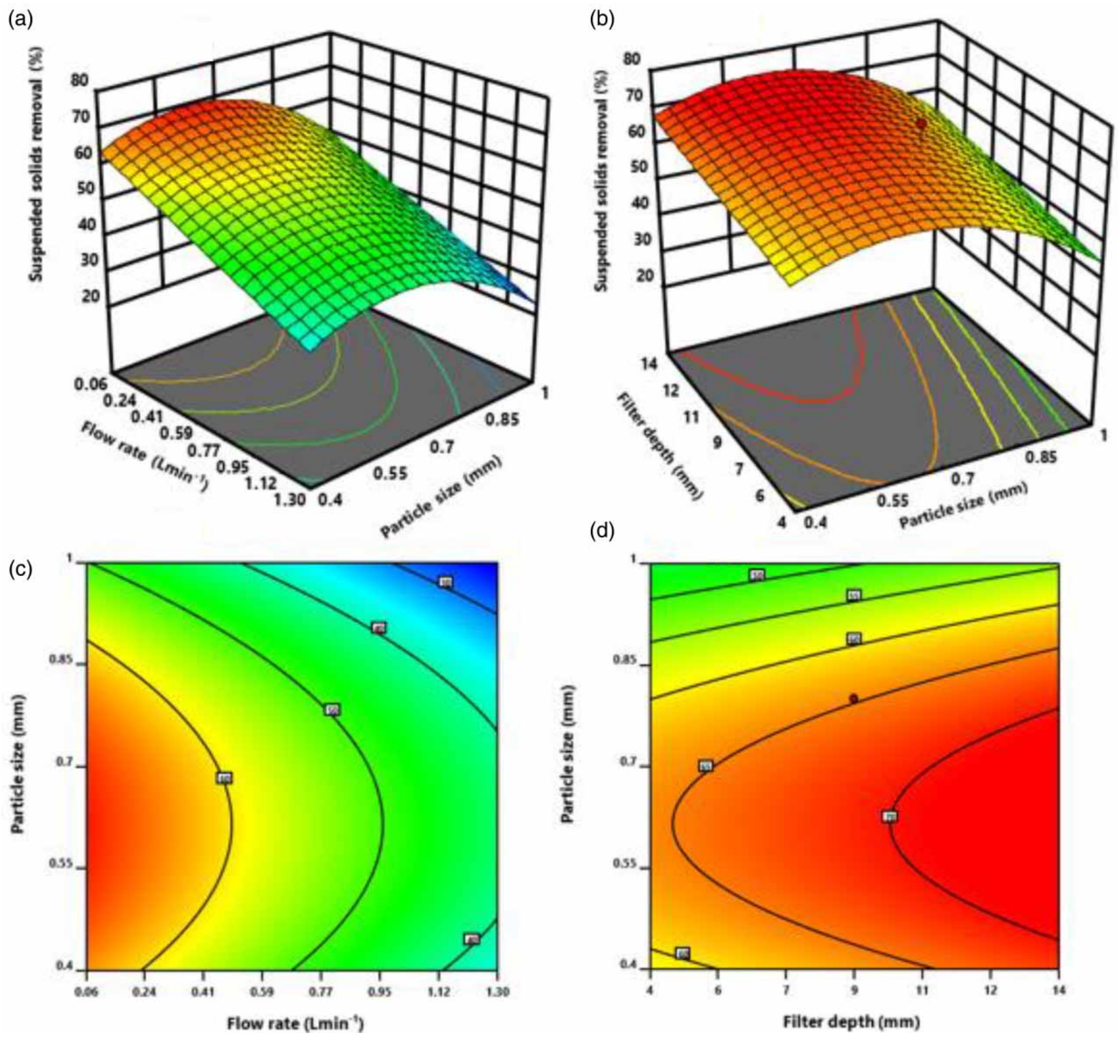

Figure 6 | Three- and two-dimensional response surface plots of suspended solids removal. (a) Effect of particle size, flow rate, and filter depth fixed at 9 cm. (b) Effect of particle size, filter depth, and flow rate fixed at 0.65 $Lmin^{-1}$. Two-dimensional contour plots of suspended solids showing (c) interaction of particle size and flow rate (d) interaction of particle size and filter depth.

predictive capability of the developed models, or else the model is negated. In this study, the mean experimental values corresponding to each of the responses lie between 95% PI low and 95% PI high (Table 8), suggesting that the developed models were valid.

The optimal solution obtained using RSM in this study is at the boundaries of the design space used for the study. The results serve to confirm that a fine filter media, slowest wastewater delivery into the filtration system and biggest depth of filter media would result in the highest removal of turbidity and TSS. It is possible that extending the boundaries could actually improve the solution. The challenge is that such an approach would lack practical significance in the sense that for very fine roughing filter media, turbidity removal will be high, but the filtration rate would practically be insignificant. A supply pump of much lower flow rate will be required. Frequent replacement of filter media would be expected. In comparison to Olupot *et al.* (2021), these results present an improvement, with potential to increase the filter runs of the downstream filtration units of an onsite recirculation system.

3.8. Performance evaluation of filtration system with optimum parameters

Analyses of handwashing wastewater after clarification using the roughing filter with optimum parameters revealed reduction efficiencies of 56, 20, 53, 32, and 5% for apparent colour, true colour, turbidity, BOD_5, and COD, respectively (see Table 9).

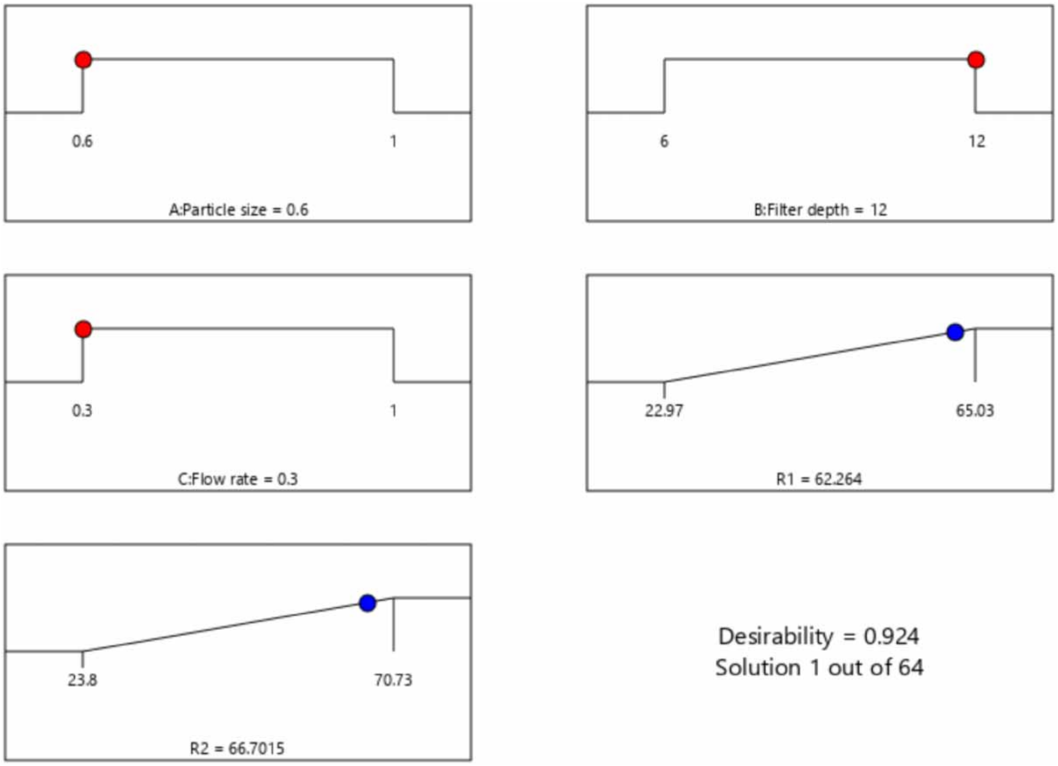

Figure 7 | Ramp function graph of desirability as suggested by the Design-Expert software.

Table 8 | Validation experiments for the proposed models

	Model for turbidity removal (%)	Model for suspended solids removal (%)
95% PI low	37.89	43.78
95% PI high	55.12	59.76
Mean experimental value	55.02	52.51
Predicted value	62.26	66.70

Table 9 | Quality of handwashing wastewater and that of water treated using the optimized roughing filtration system

	Water quality parameters					
Water type	**pH**	**Apparent colour (PtCo)**	**True colour (PtCo)**	**Turbidity (NTU)**	**BOD_5 (mgL^{-1})**	**COD (mgL^{-1})**
Handwashing wastewater	6.76	8,352	7,378	716	417	799
Treated water[a]	6.87 ± 0.07	3,644 ± 316.08	5,916 ± 25.04	337.00 ± 7.87	284.75 ± 66.51	757.50 ± 24.77

Note: [a]implies water treated by the roughing filtration system under optimized parameters.

The roughing system reported in Olupot *et al.* (2021) used similar media as used in this study. The removals of turbidity and TSS were 9–13 and 10–14%, respectively. This study therefore presents an advancement and adoption of this modification may result in significant increase in filter runs of the slow sand filtration systems downstream, thus reducing on the frequency of replacements of filter media cartridges.

Relatively low removal efficiencies by the optimized roughing filters have also been reported elsewhere, for instance, when treating effluents with high turbidity such as palm oil influent (Dashti *et al.* 2021), household greywater (Bahrami *et al.* 2020), river water (Cahyana *et al.* 2021), and dam water after a heavy storm (Hasnain & Khan 2014). The COD, BOD_5 and turbidity values obtained in this study are all less than those reported by Amiri *et al.* (2019) and Bahrami *et al.* (2020) for handwashing wastewater. These variations could be attributed to the fact that wastewater for the two cited studies was picked from residential indoor facilities as opposed to community open areas for this study.

To overcome the relatively low removal efficiencies by roughing filters, filtration media materials with superior adsorption and/or filtration properties such as plastic and coconut fibers (Hashimoto *et al.* 2019), anthracite (Karki & Amatya 2020), broken burnt bricks and agricultural residues (Nkwonta & Ochieng 2009) as well as zeolite (Al-Zou'by *et al.* 2017) could replace silica and gravel. Additionally, turbidity, TSS, and colour removal by roughing filters could be enhanced by introducing a coagulant in the raw wastewater prior to its filtration (Hasnain & Khan 2014; Hashimoto *et al.* 2019). These options were not explored in this study.

4. CONCLUSION

Optimization studies were done on finer filter sand media material on the assumption that the handwashing wastewater does not contain larger solids materials that would otherwise need to be trapped and stored in gravel and/or in the filter medium of intermediate size. The study variables were particle size, filter depth, and flow rate, which ranged from 0.6 to 1.0 mm, 6.0 to 12.0 cm, and 0.3 to 1.0 $Lmin^{-1}$, respectively. The optimum filtration parameters were found to be; filter media particle size (0.6 mm), filter depth (12 cm), and flow rate (0.3 $Lmin^{-1}$). At these optimum conditions, the model predicted removal efficiencies of 62 and 67%, which were experimentally validated to be 55 and 53% for turbidity and suspended solids, respectively. Furthermore, the removal efficiency of the roughing filter towards apparent colour, true colour, BOD_5 and COD from handwashing wastewater at the obtained optimal conditions were found to be 56, 20, 32, and 5%, respectively. Much as turbidity in the filtered water was $>$50 NTU, the developed roughing filter as a pretreatment option reduced the overall pollutant load in raw wastewater. This would thus enhance the performance of the subsequent treatment stages, such as slow sand filtration and adsorption by activated carbon.

ACKNOWLEDGEMENTS

Technical support from Mr Wabwire Andrew and Ms Rita Nakazibwe at the Department of Mechanical Engineering and Department of Civil and Environmental Engineering, Makerere University, respectively, is gratefully acknowledged.

FUNDING

This research was made possible with support from the Volkswagen Foundation, Grant 96659–1.

DATA AVAILABILITY STATEMENT

All relevant data are included in the paper or its Supplementary Information.

CONFLICT OF INTEREST

The authors declare there is no conflict.

REFERENCES

Aba, L., Prasetyo, A., Ilmawati, W. O. S., Ahmad, L. O. & Sahidin, L. O. 2019 Reduction of iron and manganese concentration in dug well water by using Moramo beach sand as filter media. *J. Phys. Conf. Ser.* **1153**. https://doi.org/10.1088/1742-6596/1153/1/012078.

Alftessi, S. A., Othman, M. H. D., Adam, M. R., Farag, T. M., Ismail, A. F., Rahman, M. A., Jaafar, J., Habib, M. A., Raji, Y. O. & Hubadillah, S. K. 2021 Novel silica sand hollow fibre ceramic membrane for oily wastewater treatment. *J. Environ. Chem. Eng.* **9**, 104975. https://doi.org/10.1016/j.jece.2020.104975.

Alim, M. A., Ashraf, A. A., Rahman, A., Tao, Z., Roy, R., Khan, M. M. & Shirin, S. 2021 Experimental investigation of an integrated rainwater harvesting unit for drinking water production at the household level. *J. Water Process Eng.* **44**, 102318. https://doi.org/https://doi.org/10.1016/j.jwpe.2021.102318.

Al-Zou'by, J. Y., Al-Zboon, K. K. & Al-Tabbal, J. A. 2017 Low-cost treatment of grey water and reuse for irrigation of home garden plants. *Environ. Eng. Manage. J.* **16**, 351–359. https://doi.org/10.30638/eemj.2017.035.

Amiri, M. J., Bahrami, M., Badkouby, M. & Kalavrouziotis, I. K. 2019 Greywater treatment using single and combined adsorbents for landscape irrigation. *Environ. Process* **6**, 43–63. https://doi.org/10.1007/s40710-019-00362-1.

Amuakwa-Mensah, F., Afua, R. & Kofi, P. 2021 COVID-19 and handwashing: implications for water use in Sub-Saharan Africa. *Water Resour. Econ.* **36**. https://doi.org/10.1016/j.wre.2021.100189.

Antony, J. 2014 A systematic methodology for design of experiments. In: *Design of Experiments for Engineers and Scientists* (Antony, J., ed.). Elsevier Ltd, pp. 33–50. https://doi.org/10.1016/B978-0-08-099417-8.00004-3.

APHA/AWWA/WEF. 2012 *Standard Methods for the Examination of Water and Wastewater*, 22nd edn. American Public Health Association (APHA), American Water Works Association (AWWA) and Water Environment Federation (WEF), Washington, DC, USA.

Bahrami, M., Amiri, M. J. & Badkubi, M. 2020 Application of horizontal series filtration in greywater treatment: a semi-industrial study. *Aust. J. Water Resour.* **24**, 236–247. https://doi.org/10.1080/13241583.2020.1824610.

Bakare, B. F., Mtsweni, S. & Rathilal, S. 2019 Pilot study of a horizontal roughing filtration system treating greywater generated from a peri-urban community in Durban, South Africa. *J. Water Reuse Desalin.* **9**, 330–337. https://doi.org/10.2166/wrd.2019.055.

Barişçi, S. & Turkay, O. 2016 Domestic greywater treatment by electrocoagulation using hybrid electrode combinations. *J. Water Process Eng.* **10**, 56–66. https://doi.org/10.1016/j.jwpe.2016.01.015.

Bukuluki, P., Mwenyango, H., Katongole, S. P., Sidhva, D. & Palattiyil, G. 2020 The socio-economic and psychosocial impact of COVID-19 pandemic on urban refugees in Uganda. *Soc. Sci. Humanities Open* **2**, 100045. https://doi.org/10.1016/j.ssaho.2020.100045.

Cahyana, G. H., Firdaus, A. R. & Mulyani, T. 2021 Effectiveness of combined up-flow roughing filter and up-flow slow sand filter to reduce turbidity in Citarum water as a source of drinking water. *IOP Conf. Ser. Earth Environ. Sci.* **896**. https://doi.org/10.1088/1755-1315/896/1/012020.

Chang, L., Wang, C. J. & Scd, T. C. 2022 Childhood handwashing habit formation and later COVID-19 preventive practices: a cohort study. *Acad. Pediatr.* https://doi.org/10.1016/j.acap.2022.05.014.

Cleary, A. S. 2005 *Sustainable Drinking Water Treatment for Small Communities Using Multi-Stage Slow Sand Filtration*. University of Waterloo, Waterloo, ON, Canada.

Dashti, A. F., Aziz, H. A., Adlan, M. N. & Ibrahim, A. H. 2019 Calcined limestone horizontal roughing filter for treatment of palm oil mill effluent polishing pond. *Int. J. Environ. Sci. Technol.* **16**, 6419–6430. https://doi.org/10.1007/s13762-019-02467-4.

Dashti, F. A., Abdul Aziz, H., Adlan, M. N. & Ibrahim, A. H. 2021 Effect of calcined limestone on the performance of roughing filter for turbidity removal of palm oil mill effluent. *J. Hazard. Toxic Radioact. Waste* **25**. https://doi.org/10.1061/(asce)hz.2153-5515.0000607.

El-taweel, G. E. & Ali, G. H. 2000 Evaluation of roughing and slow sand filters for water treatment. *Water Air Soil Pollut.* **120**, 21–28.

Hashimoto, Y., Takashima, H. & Jayamohan, S. 2019 Application of roughing filter to pre-treat 1,000 NTU raw water for slow sand filter. *Water Pract. Technol.* **14**, 355–364. https://doi.org/10.2166/wpt.2019.021.

Hasnain, G. & Khan, Z. 2014 Treatment of high turbidity water through plain and coagulated up-flow roughing filter. *Desalin. Water Treat.* **52**, 1035–1043. https://doi.org/10.1080/19443994.2013.826772.

Karki, B. K. & Amatya, I. M. 2020 A comparative study of water turbidity removal efficiency of anthracite and gravel in roughing filter. *J. Innovation Eng. Educ.* **3**, 42–49. https://doi.org/10.3126/jiee.v3i1.34323.

Khan, Z. & Farooqi, R. 2011 Roughing filtration as an effective pre-treatment system for high turbidity water. *Water Sci. Technol.* **64**, 1419–1427. https://doi.org/10.2166/wst.2011.317.

Lee, S.-H. & Jayalath, J. 1998 Performance evaluation of horizontal flow roughing filter as a pretreatment system. *KSCE J. Civ. Eng.* **2**, 187–193.

Logsdon, G. S., Kohne, R., Abel, S. & LaBonde, S. 2002 Slow sand filtration for small water systems. *J. Environ. Eng. Sci.* **1**, 339–348. https://doi.org/10.1139/S02-025.

Luna-Guevara, J., Arenas-Hernandez, M., Martínez de la Peña, C., Silva, L. & Luna-Guevara, L. 2019 The role of pathogenic *E. coli* in fresh vegetables: behavior, contamination factors, and preventive measures. *Int. J. Microbiol.* **2019**, 1–10.

Maciel, P. M. F., Fava, N. d. M. N., Lamon, A. W., Fernandez-Ibañez, P., Byrne, J. A. & Sabogal-Paz, L. P. 2021 Household water purification system comprising cartridge filtration, UVC disinfection and chlorination to treat turbid raw water. *J. Water Process Eng.* **43**. https://doi.org/10.1016/j.jwpe.2021.102203.

Matuzahroh, N., Fitriani, N., Ardiyanti, P. E., Kuncoro, E. P., Budiyanto, W. D., Isnadina, D. R. M., Wahyudianto, F. E. & Mohamed, R. M. S. R. 2020 Behavior of schmutzdecke with varied filtration rates of slow sand filter to remove total coliforms. *Heliyon* **6**, e03736. https://doi.org/10.1016/j.heliyon.2020.e03736.

Menya, E., Olupot, P. W., Storz, H., Lubwama, M., Kiros, Y. & John, M. J. 2019 Optimization of pyrolysis conditions for char production from rice husks and its characterization as a precursor for production of activated carbon. *Biomass Convers. Biorefin.* https://doi.org/10.1007/s13399-019-00399-0.

Munasir, M., Triwikantoro, T., Zainuri, M. & Darminto, D. 2015 Synthesis of SiO2 nanopowders containing quartz and cristobalite phases from silica sands. *Mater. Sci. Pol.* **33**, 47–55. https://doi.org/10.1515/msp-2015-0008.

Mushila, C., Ochieng, G., Otieno, F. & Shitote, S. M. 2016 Performance of horizontal-flow roughing filter units (HRF) under varied raw water conditions in Kenya. *J. Glob. Resour.* **2**, 136–144.

NEMA 1999 *The National Environment (Standards for Discharge of Effluent into Water or on Land) Regulations, S.I, National Environment Act, Cap 153.*

Nguyen, M. T., Allemann, L., Ziemba, C., Larivé, O., Morgenroth, E. & Julian, T. R. 2017 Controlling bacterial pathogens in water for reuse: treatment technologies for water recirculation in the Blue Diversion Autarky Toilet. *Front. Environ. Sci.* **5**, 1–13. https://doi.org/10.3389/fenvs.2017.00090.

Nkwonta, O. 2010 A comparison of horizontal roughing filters and vertical roughing filters in wastewater treatment using gravel as a filter media. *Int. J. Phys. Sci.* **5**, 1240–1247.

Nkwonta, O. & Ochieng, G. 2009 Roughing filter for water pre-treatment technology in developing countries: a review. *Int. J. Phys. Sci.* **4**, 455–463.

Nkwonta, O. I., Olufayo, O. A., Ochieng, G. M., Adeyemo, J. A. & Otieno, F. A. O. 2010 Turbidity removal: gravel and charcoal as roughing filtration media. *S. Afr. J. Sci.* **106**, 1–5. https://doi.org/10.4102/sajs.v106i11/12.196.

Nouri, J., Mahvi, A. H., Saeedi, R., Dindarloo, K., Rafiee, M. & Dobaradaran, S. 2008 Purification and removal of Ascaris and Fasciola hepatica eggs from drinking water using roughing filters. *Korean J. Chem. Eng.* **25**, 501–504.

Olupot, W. P., Menya, E., Jjagwe, J., Wakatuntu, J., Kavuma, T., Wabwire, A., Kavuma, S., Okodi, S., Nabuuma, B. & Mpagi, H. 2021 Development and appraisal of handwash-wastewater treatment system for water recycling as a resilient response to COVID-19. *J. Environ. Chem. Eng.* **9**, 106113.

Oxfam 2001 *Oxfam Guidelines for Water Treatment in Emergencies, Public Health Engineering Team*. UK.

Oyedotun, T. D. T. 2018 X-ray fluorescence (XRF) in the investigation of the composition of earth materials: a review and an overview. *Geol. Ecol. Landscapes* **2**, 148–154. https://doi.org/10.1080/24749508.2018.1452459.

Ratna, R. V. 2019 Economic analysis of health impacts in developing countries. *Encycl. Environ. Health*, 221–230. https://doi.org/10.1016/B978-0-12-409548-9.10939-X.

Rey, V., Ríos, C. A., Vargas, L. Y. & Valente, T. M. 2021 Use of natural zeolite-rich tuff and siliceous sand for mine water treatment from abandoned gold mine tailings. *J. Geochem. Explor.* **220**, 106660. https://doi.org/10.1016/j.gexplo.2020.106660.

Samayamanthula, D. R., Sabarathinam, C. & Bhandary, H. 2019 Treatment and effective utilization of greywater. *Appl. Water Sci.* **9**, 1–12. https://doi.org/10.1007/s13201-019-0966-0.

Setiati, N. R. 2017 The potential use of silica sand as nanomaterials for mortar. *AIP Conf. Proc.* **1903**. https://doi.org/10.1063/1.5011549.

Subramanian, P. S. G., Raj, A. V., Jamwal, P., Connelly, S., Yeluripati, J., Richards, S., Ellis, R. & Rao, L. 2020 Decentralized treatment and recycling of greywater from a school in rural India. *J. Water Process Eng.* **38**, 101695. https://doi.org/10.1016/j.jwpe.2020.101695.

Talib, N. A. A., Salam, F., Yusof, A., Alang, A. & Sulaiman, Y. 2017 Optimization of peak current of poly(3,4-ethylenedioxythiophene)/multi-walled carbon nanotube using response surface methodology/ central composite design. *RSC Adv.* **7**, 11101–11110. https://doi.org/10.1039/C6RA26135C.

Wegelin, M. 1996 *Surface Water Treatment by Roughing Filters: A Design, Construction and Operation Manual*. SANDEC Report No 2/96.

Wegelin, M. & Schertenleib, R. 1993 *Roughing Filters for Water Treatment*. IRCWD News.

WHO 2008 *Guidelines for Drinking-Water Quality: Incorpotating 1st and 2nd Addenda*. Vol. 1, Recommendations–Third Edition. World Health Organization, Geneva, Switzerland.

WHO 2020 *Interim Guidance April 2020: Water, Sanitation, Hygiene and Waste Management for the COVID-19 virusInterim Guidance April 2020*. World Health Organization, Geneva, Switzerland, pp. 1–9.

Wong, R., Grullon, J. R. & Lovier, M. A. 2022 COVID-19 risk factors and predictors for handwashing, masking, and social distancing among a national prospective cohort of U.S. older adults. *Public Health*. https://doi.org/10.1016/j.puhe.2022.08.002.

Ziemba, C., Larivé, O., Reynaert, E. & Morgenroth, E. 2018 Chemical composition, nutrient-balancing and biological treatment of hand washing greywater. *Water Res.* **144**, 752–762. https://doi.org/10.1016/j.watres.2018.07.005.

First received 20 June 2022; accepted in revised form 21 October 2022. Available online 2 November 2022